NEURO

Quantitative regional validation of the visual rating scale for posterior cortical atrophy

Christiane Möller · Wiesje M. van der Flier · Adriaan Versteeg · Marije R. Benedictus · Mike P. Wattjes · Esther L. G. M. Koedam · Philip Scheltens · Frederik Barkhof · Hugo Vrenken

Abstract

Objectives Validate the four-point visual rating scale for posterior cortical atrophy (PCA) on magnetic resonance images (MRI) through quantitative grey matter (GM) volumetry and voxel-based morphometry (VBM) to justify its use in clinical practice.

Methods Two hundred twenty-nine patients with probable Alzheimer's disease and 128 with subjective memory complaints underwent 3T MRI. PCA was rated according to the visual rating scale. GM volumes of six posterior structures and the total posterior region were extracted using IBASPM and compared among PCA groups. To determine which anatomical regions contributed most to the visual scores, we used binary logistic regression. VBM compared local GM density among groups.

Results Patients were categorised according to their PCA scores: PCA-0 ($n=122$), PCA-1 ($n=143$), PCA-2 ($n=79$), and PCA-3 ($n=13$). All structures except the posterior cingulate differed significantly among groups. The inferior parietal gyrus volume discriminated the most between rating scale levels. VBM showed that PCA-1 had a lower GM volume than PCA-0 in the parietal region and other brain regions, whereas between PCA-1 and PCA-2/3 GM atrophy was mostly restricted to posterior regions.

Conclusions The visual PCA rating scale is quantitatively validated and reliably reflects GM atrophy in parietal regions, making it a valuable tool for the daily radiological assessment of dementia.

Key Points
• *Visual rating scale reflects grey matter atrophy in posterior brain regions.*
• *Different PCA scores corresponded well to different quantitative degrees of atrophy.*
• *Inferior parietal gyrus volume influenced assessment based on the visual rating scale.*
• *This simple visual rating scale makes it useful for radiological dementia assessment.*

C. Möller (✉) · W. M. van der Flier · M. R. Benedictus ·
E. L. G. M. Koedam · P. Scheltens
Alzheimer Center & Department of Neurology,
VU University Medical Center, Neuroscience Campus Amsterdam,
P.O. Box 7057, 1007 MB Amsterdam, The Netherlands
e-mail: c.moeller@vumc.nl

A. Versteeg · M. P. Wattjes · F. Barkhof · H. Vrenken
Department of Radiology & Nuclear Medicine,
VU University Medical Center, Neuroscience Campus Amsterdam,
P.O. Box 7057, 1007 MB Amsterdam, The Netherlands

W. M. van der Flier
Department of Epidemiology & Biostatistics,
VU University Medical Center, Neuroscience Campus Amsterdam,
P.O. Box 7057, 1007 MB Amsterdam, The Netherlands

H. Vrenken
Department of Physics & Medical Technology,
VU University Medical Center, Neuroscience Campus Amsterdam,
P.O. Box 7057, 1007 MB Amsterdam, The Netherlands

Abbreviations and acronyms

AD	Alzheimer's disease
PCA	Posterior cortical atrophy
VBM	Voxel-based morphometry
MTA	Medial temporal lobe atrophy
GCA	Global cortical atrophy
TIV	Total intracranial volume
FWE	Family-wise error
ROI	Region of interest
WMH	White matter hyperintensities
CSF	Cerebrospinal fluid
WM	White matter
GM	Grey matter

Introduction

The most salient characteristic of Alzheimer's disease (AD) on magnetic resonance imaging (MRI) is atrophy of the medial temporal lobe, including the hippocampus [1]. However, atrophy may also occur in the posterior cortex and early posterior cortical involvement is emerging as an important aspect of AD [2–7]. Posterior cortical atrophy (PCA) is often evident from visual inspection on structural MRI. We recently proposed a visual rating scale for assessing the degree of PCA [8]. This scale was found to be robust, reproducible, and easily applicable in a clinical setting [7, 8].

To establish the validity of this visual PCA rating scale and thereby determine whether its use in clinical practice is justified, it should be compared against quantitative brain volumetry, as has been done previously for other visual rating scales [9–11]. This issue has partially been addressed by comparing PCA scores with the manually determined volumes of the posterior cingulate gyrus, a single structure within the posterior region [7]. The visual rating scale for PCA however covers a larger anatomical area and full validation against volumetry is lacking.

Therefore, in the current study, we provide a validation covering the entire anatomical region of interest. We assessed the mutual discriminatory value of the possible scores of the visual PCA rating scale at three different levels of anatomical detail: the entire parietal brain region, the individual anatomical subregions, and in much finer detail using voxel-based morphometry (VBM). Finally, we assessed which anatomical regions contribute most to the discrimination between PCA scores.

Materials and methods

Patients

The study was approved by the local institutional medical ethics committee. All patients gave written informed consent.

We included 398 patients with probable AD or subjective complaints from our memory clinic-based Amsterdam Dementia Cohort. All patients visited the Alzheimer Centre or the Department of Internal Medicine (COGA) of the VU University Medical Centre (VUmc) between August 2008 and January 2011 and underwent a standardised 1-day assessment including MRI. Diagnoses of probable AD were made in a multidisciplinary consensus meeting according to the NIA-AA criteria [12]. Patients with normal clinical investigations [i.e. not fulfilling criteria for mild cognitive impairment (MCI) [13] or any major psychiatric disorder] were labelled as having subjective memory complaints. For inclusion in the present study a three-dimensional T1-weighted sequence (3D T1) and a 3D fluid-attenuated inversion-recovery (FLAIR) sequence acquired

during the same session were required. Exclusion criteria were (1) poor MR image quality and/or large image artefacts ($n = 4$), (2) an asymmetric PCA visual rating score ($n = 34$), and (3) gross abnormalities other than atrophy, including severe white matter hyperintensities (WMH) ($n = 3$) as defined below.

MRI acquisition and review

Magnetic resonance imaging was performed on a 3.0-T whole-body MRI system (SignaHDxt, GE Healthcare, Milwaukee, WI, USA) using an eight-channel head coil with foam padding to restrict head motion. Imaging included a whole-brain 3D T1 fast spoiled gradient echo sequence (FSPGR; TR 708 ms, TE 7 ms, flip angle 12°, 180 sagittal slices, field of view 250 mm, slice thickness 1 mm, voxel size $0.98 \times 0.98 \times 1$ mm) used for VBM and for the visual rating. A 3D FLAIR sequence (TR 8,000 ms, TE 125 ms, 132 sagittal slices, field of view 250 mm, slice thickness 1.2 mm, TI = 2349 ms) was acquired for visual rating of WMH. MR images were reviewed for brain abnormalities other than atrophy by experienced neuroradiologists (FB, 20 years' experience; MPW, 10 years' experience). WMHs were rated on 3-mm axial reformats of the 3D FLAIR sequences (by FB and MPW) with the Fazekas scale [14], a four-point rating of the overall presence of WMH. Subjects with a maximum Fazekas scale score were excluded.

Visual rating of PCA

Details about rating of posterior cortical atrophy can be found in the original paper about the visual rating scale [8]. In short, PCA was rated with a 4-point scale with PCA-0 = no atrophy, PCA-1 = minimal atrophy, PCA-2 = moderate atrophy, and PCA-3 = severe atrophy based on multiplanar reconstructions (sagittal, coronal, axial) of the 3D T1 and 3D FLAIR images (Fig. 1). Rating of PCA takes approximately 2 min per patient for a skilled rater. All imaging was rated by the same rater (MB, 6 months' experience). Each tenth acquisition was rated in consensus with an experienced neuroradiologist (MPW, 10 years' experience). When there was doubt about appropriate scoring, imaging was discussed in a consensus meeting with MPW. Both raters were blinded to the subjects' age, sex, and diagnosis. Intra-rater reliability was determined for 60 acquisitions from the data set and was very good with a weighted kappa (quadratic weights) of 0.95 for left and right scores. Inter-rater reliability between MB and MPW was also very good with a weighted kappa (quadratic weights) of 0.85 for left and right scores. Patients were categorised into groups based on the PCA scores of their imaging. MRIs were also rated in terms of medial temporal lobe atrophy (MTA) (according to the five-point visual rating scale) [9] and global cortical atrophy (GCA) (according to the four-point visual rating scale) [9, 15].

Fig. 1 Scoring of the visual rating scale for posterior cortical atrophy (PCA). In sagittal orientation, widening of the posterior cingulate sulcus (*PCS*) and parieto-occipital sulcus (POS) and atrophy of the precuneus (PRE) were evaluated. In axial orientation, the widening of the posterior cingulate sulcus and sulcal dilation in the parietal lobes (PAR) were evaluated. In coronal orientation, the widening of the posterior cingulate sulcus and sulcal dilation in the parietal lobes were evaluated. From *left* to *right* sagittal 3D T1, axial 3D FLAIR, and coronal 3D T1 reconstructions with **a**: 0 = no atrophy (38-year-old man with subjective memory complaints); **b**: 1 = minimal atrophy (73-year-old woman with Alzheimer's disease [AD]); **c**: 2 = moderate atrophy (68-year-old woman with AD); **d**: 3 = severe atrophy (62-year-old woman with AD)
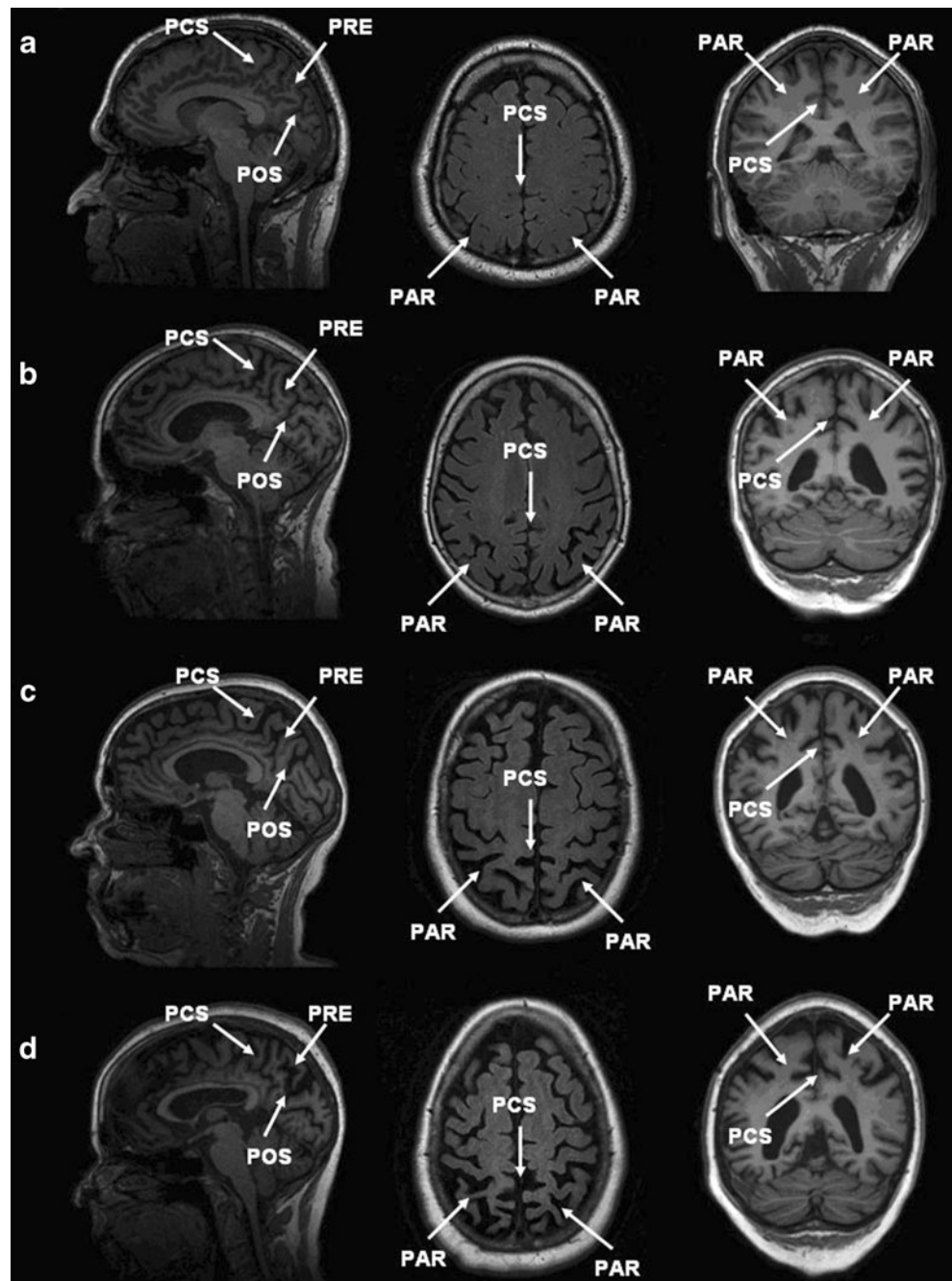
Tissue type segmentation

DICOM images of the FSPGR sequence were corrected in three dimensions for gradient non-linearity distortions and converted to the Nifti format. The linear transformation matrix to the MNI space was calculated using FSL-FLIRT [16] and used to place the image coordinate origin (0,0,0) on the anterior commissure using the Nifti s-form.

The structural 3D T1 images were analysed using Statistical Parametric Mapping (SPM8; Functional Imaging Laboratory, University College London, London, UK) implemented in MATLAB 7.12 (MathWorks, Natick, MA, USA). First, SPM8 was used to automatically quantify probabilities of grey matter (GM), white matter (WM), and cerebrospinal fluid (CSF) for each voxel of each native image. Total intracranial volume (TIV) was calculated by summing up the native space volumes of GM, WM, and CSF segmentations.

Volumetry of regions of interest

We calculated the total GM volumes of six structures covered by the visual rating scale for PCA: bilateral posterior cingulate,

postcentral gyrus, superior and inferior parietal gyrus, and angular gyrus and precuneus, as follows. Using the fully automated "Individual Brain Atlases as implemented in the Statistical Parametric Mapping" (IBASPM) toolbox [17], (http://www.thomaskoenig.ch/Lester/ibaspm.htm), based on SPM software (http://www.fil.ion.ucl.ac.uk/spm), for each participant, each voxel of the native GM density maps was assigned to one of the 84 predefined cerebral GM structures in the Automatic Anatomic Labelling (AAL) atlas by applying the inverse of the image transformation obtained in the VBM normalisation process (details below) [18]. Segmentation results were visually inspected for accuracy, and none had to be discarded. The GM volume (cm^3) of each of the six structures covered by the PCA rating scale was estimated using the IBASPM volume statistic function. GM volumes for the left and right parts of each structure were summed and transferred to SPSS. The total GM volume of the whole parietal region of interest (ROI) was calculated as the sum of the volumes of the six structures.

Statistical analysis of volumes

Statistical analyses of clinical data were performed using SPSS 20.0 for Windows (IBM SPSS Statistics, Somers, NY, USA), using Student's t-tests, Mann-Whitney U-tests, and Pearson's chi-squared tests to compare groups where appropriate. To test if the total GM volume of the whole parietal ROI (dependent variable) differed among the four PCA scores (independent variable), we used analysis of variance (ANOVA) with TIV as a covariate. As the raters of the degree of PCA were blinded to the subjects' age and sex, and therefore these did not influence the rating, these two variables were not included as covariates. Bonferroni post-hoc tests were conducted. Additionally, we investigated whether the GM volume of the six structures separately (dependent variables) differed among the four PCA scores (fixed factor) using a multivariate model (MANOVA) with TIV as a covariate. Partial eta squared (η_p^2) values were calculated to estimate the effect sizes. To assess which anatomical regions contributed most to a higher score on the visual PCA rating scale, we conducted two binary logistic regression analyses between PCA groups (dependent variable): first, between PCA-0 and PCA-1; second, between PCA-1 and combined PCA-2/PCA-3. For these logistic regression analyses, volumes of the six structures were transformed to z-scores and included as independent variables. PCA scores were coded such that odds ratios reflected the increased risk associated with a higher PCA-score per standard deviation smaller volume of a specific structure. We used the forward conditional method. The level of significance was set at $P < 0.05$.

Voxel-based morphometry

Voxel-based morphometry was performed using a modified pipeline in SPM8 (Functional Imaging Laboratory, University College London, London, UK). After tissue segmentation, images were rigidly aligned. Next, a "DARTEL" GM template of all acquisitions was created by non-linearly aligning the GM images of all participants to a common space [19]. DARTEL is an average group-specific template to increase the accuracy of inter-subject alignment. Native GM and WM segmentations were spatially normalised to the DARTEL template by applying the individual flow fields of all acquisitions, using modulation to compensate for volume changes resulting from compression and/or expansion. Images were smoothed using a 4-mm full-width at half maximum (FWHM) isotropic Gaussian kernel. Images were visually inspected at every processing step.

To localise GM differences, voxelwise statistical comparisons between groups were made using a full factorial design with PCA as a factor with independent levels, unequal variance, TIV as a covariate, an absolute threshold of 0.2, and implicit masking. The following post-hoc pairwise comparisons were made: PCA-0 was compared with PCA-1 and with PCA-2; PCA-1 was compared with PCA-2 and PCA-3 together (PCA-2/3). The statistical significance threshold was set to $P < 0.05$ with family-wise error correction (FWE) at the voxel level.

Results

Images of 357 patients (229 AD patients, 128 patients with subjective memory complaints) were available for analysis. Patients were categorised according to PCA rating scores, resulting in a study sample of 122 patients with PCA-0, 143 patients with PCA-1, 79 patients with PCA-2, and 13 patients with PCA-3.

Demographic data according to PCA groups are summarised in Table 1. AD patients were predominantly classified as PCA-1 (47 %), whereas most of the patients with subjective memory complaints (66 %) were in the group PCA-0. MTA and GCA scores were lowest in PCA-0 and highest in PCA-3 group ($P < 0.001$). Patients with any degree of PCA had lower total brain volume (TBV) than patients categorised in PCA-0 ($P < 0.001$).

Analysis of variance (ANOVA) showed that total GM volume of the whole parietal ROI differed among the four PCA groups ($P < 0.001$) with the largest volumes in PCA-0 and the smallest volumes in PCA-3 (Table 2; Fig. 2). MANOVA for the six posterior cortical structures revealed a significant main effect of the PCA rating scale: All structures except the posterior cingulate differed among the four PCA groups (posterior cingulate gyrus: $P = 0.054$, $\eta_p^2 = 0.021$; postcentral gyrus: $P < 0.001$, $\eta_p^2 = 0.30$; superior parietal gyrus: $P < 0.001$, $\eta_p^2 = 0.29$; inferior parietal gyrus: $P < 0.001$, $\eta_p^2 = 0.35$; angular gyrus: $P < 0.001$, $\eta_p^2 = 0.25$; precuneus: $P < 0.001$, $\eta_p^2 = 0.30$). Bonferroni-corrected post-hoc pairwise comparisons revealed that the volumes of these five structures (all except the posterior cingulate gyrus) differed among all PCA group pairs, except between PCA-2 and PCA-3 (Fig. 3,

Table 1 Demographic characteristics

| | Score on visual rating scale for posterior cortical atrophy | | | |
	PCA-0	PCA-1	PCA-2	PCA-3
n	122	143	79	13
Diagnosis, AD/SMC (n)^	37/85	108/35	72/7	12/1
Sex, female (n)	69 (57 %)	68 (48 %)	32 (41 %)	7 (54 %)
Age, years	62.6±8.1	67.7±8.2#	67.4±8.6#	71.6±10.1#
MMSE	25.9±4.3#	23±5	21.1±5.5##	20.5±6.4
MTA score^	0.5±0.8	1.1±0.8	1.4±0.9	1.9±1.1
GCA score^	0.2±0.4	1±0.5	1.6±0.5	2.2±0.6*
TBV (l)	1.4±0.1	1.2±0.1#	1.2±0.1#	1.1±0.1#

Values presented as mean ± standard deviation or n (%). Groups were compared using Student's t-tests, Mann-Whitney U-tests, and Pearson's chi-Squared tests where appropriate

^Differences between all groups with $P \leq 0.001$. # Difference between PCA-0 vs. PCA-1, PCA-0 vs. PCA-2, and PCA-0 vs. PCA-3 with $P \leq 0.01$. ## Difference between PCA-1 and PCA-2 with $P \leq 0.05$. *No difference between PCA-2 and PCA-3

AD, patients with Alzheimer's disease; SMC, patients with subjective memory complaints; MMSE: Mini-Mental State Examination; MTA, score on the visual rating scale for medial temporal lobe atrophy; GCA, score on the visual rating scale for global cortical atrophy; TBV, total brain volume

Table 2). The small group size of the PCA-3 group limits the statistical power of comparisons with this group.

To investigate which structures contributed most to the discrimination between scoring levels of the PCA rating scale, we used binary logistic regression. Comparing PCA-0 and PCA-1, logistic regression (stepwise forward) revealed that the inferior parietal gyrus (OR=3.7, 95 % CI=1.5–9), the precuneus (OR=2.2, 95 % CI=1.2-4.1), and the angular gyrus (OR=0.4, 95 % CI=0.2–0.9) contributed independently to a higher score. Comparing PCA-1 and PCA-2/3, the inferior parietal gyrus (OR=5.1, 95 % CI=2.3–11.6) and the angular gyrus (OR=0.5, 95 % CI=0.2–0.99) contributed the most to the higher PCA score. Odds ratios higher than 1 reflect a negative relationship between volume of the area and the PCA score, i.e., the smaller the volume of an area, the higher the odds of a higher PCA score.

Table 2 Grey matter (GM) volume of parietal structures

| Volume (cm^3) | Score on visual rating scale for posterior cortical atrophy | | | |
	PCA-0	PCA-1	PCA-2	PCA-3
Total posterior ROI^	89.2±12.9	77.4±11.1	72.1±9.2	66.3±10.6
Posterior cingulate gyrus	2.7±0.5	2.5±0.4	2.5±0.4	2.5±0.5
Postcentral gyrus^	24.4±3.5	21.5±3.1	20.2±2.6	18.2±3.7
Superior parietal gyrus^	10.8±2.1	8.9±1.8	8.2±1.5	7.3±1.7
Inferior parietal gyrus^	15.3±2.4	13.1±2.2	11.8±1.8	10.6±2
Angular gyrus^	12.0±1.7	10.6±1.6	10.0±1.5	9.5±1.4
Precuneus^	24.1±3.7	20.7±3.1	19.4±2.7	18.3±2.7

Values presented as mean ± standard deviation. (M)ANOVAs with TIV as covariate were conducted between the four PCA groups. ^Differences between all PCA groups with $P \leq 0.01$, except between PCA-2 and PCA-3

VBM results

Voxel-based morphometry analyses showed that the visual PCA rating scale discriminates well between atrophy (PCA-1, PCA-2) and no atrophy (PCA-0) in the parietal brain regions considered by the rating scale and that with increasing parietal atrophy more atrophy of the whole brain was detected. Compared with PCA-0, the PCA-1 group had less GM in the
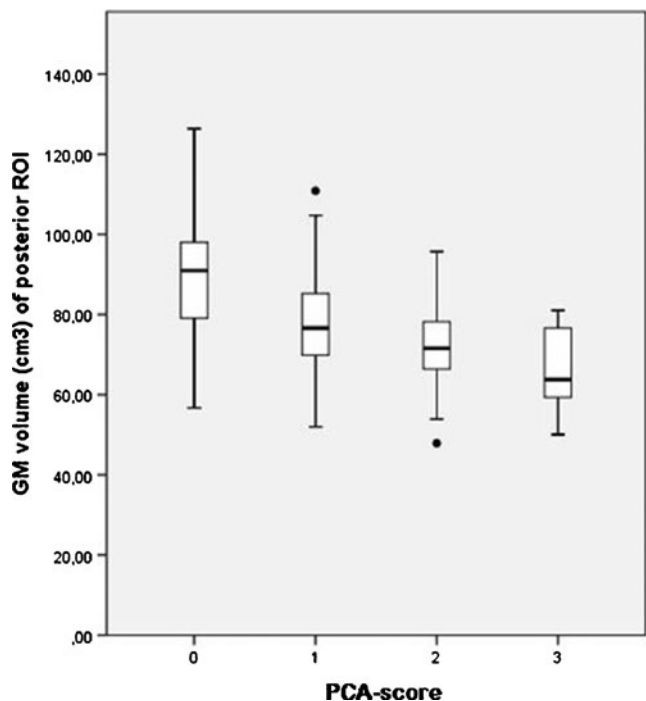

Fig. 2 Boxplot of GM volume of the whole parietal ROI of the four different PCA groups. Volumes differed significantly among all PCA groups ($P < 0.001$)

Fig. 3 Boxplots of GM volumes of the six different structures for each PCA group. Volumes of all structures differed among all PCA groups except between PCA-2 and PCA-3. The volumes of the posterior cingulate did not differ among any of the PCA groups. Coloured structures: *red*;, precuneus; *green*, superior parietal gyrus; *dark blue*, postcentral gyrus; *yellow*, inferior parietal gyrus; *light blue*, angular gyrus; *copper*, posterior cingulate gyrus
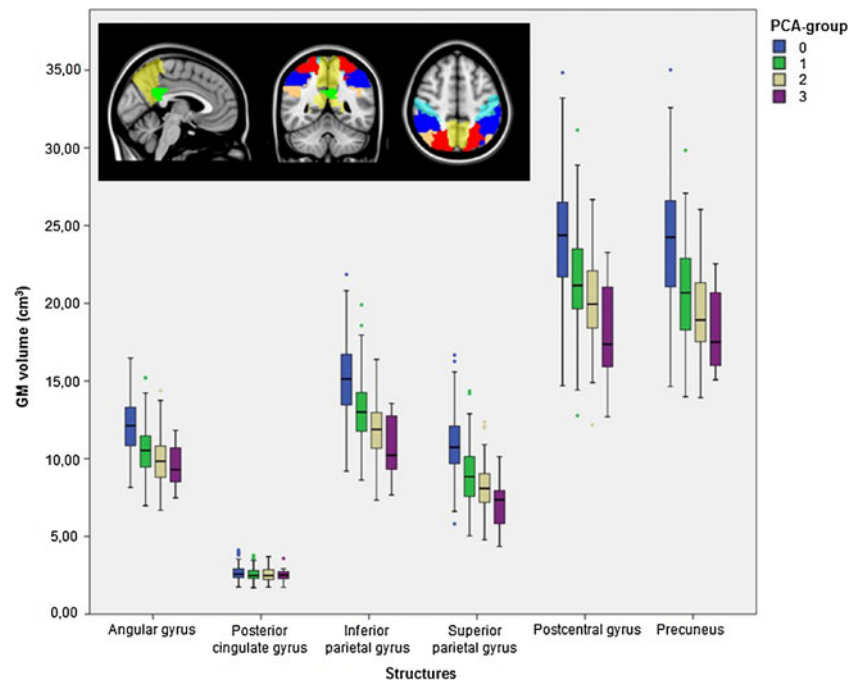
medial cingulate gyrus, middle occipital gyrus, insular cortex, hippocampus, inferior frontal gyrus, precentral gyrus, angular gyrus, and middle temporal gyrus ($P < 0.05$ FWE; Fig. 4). Compared with PCA-0, PCA-2 had less GM in the precuneus, postcentral gyrus, and cerebellum ($P < 0.05$ FWE). Compared with PCA-1, moderate to severe PCA (PCA-2/3) had less GM in the right precuneus, supplementary motor area, fusiform gyrus, and medial temporal lobe ($P < 0.05$ FWE; Fig. 4).

Discussion

We showed with volumetric analysis and VBM that the visual PCA rating scale reliably reflects GM atrophy in parietal cortical regions. There was a clear separation between brains rated as having PCA and those rated as having no atrophy.

Moreover, the different severity scores in the rating scale corresponded to different quantitative degrees of atrophy. Finally, the volume of the inferior parietal gyrus in particular affected the visual PCA scoring.

Previous studies showed that the presence of PCA may be a helpful additional imaging marker for AD, especially in patients with an early onset [3, 20], and in distinguishing AD from fronto-temporal dementia (FTD) [7, 21]. The recently developed visual rating scale for PCA detects a wide range of PCA and is a quick, reproducible, and easily applicable tool for the clinical setting [8]. However, it has not been quantitatively validated so far, which may have hampered its clinical applicability.

The current study quantitatively validated the PCA scale at three levels of anatomical detail. First, GM volumes of the entire parietal ROI covered by the scale were smaller for

Fig. 4 Voxel-wise comparisons between PCA-0 vs. PCA-1 showed that the visual PCA rating scale discriminates well between atrophy and no atrophy (*above*) as well as between minimal and moderate/severe atrophy (PCA-1 vs. PCA-2 and PCA-3, *below*). In particular, higher scores on the visual scale reflect specific atrophy of the posterior cortex. *Brighter colours* indicate higher t-values. Figures are displayed with a threshold of $P < 0.001$, uncorrected
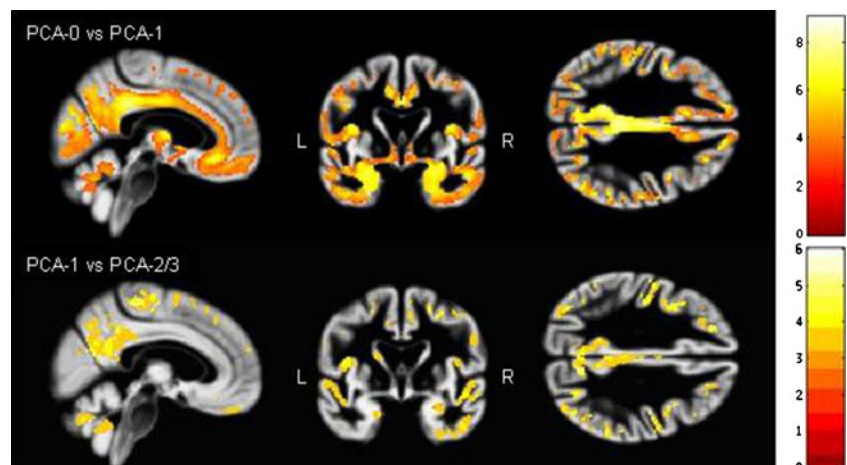
higher scores and differed significantly among all pairs of PCA groups, except between PCA-2 and PCA-3, which may be explained by insufficient power due to the small size of the PCA-3 group (13 patients). Second, the same behaviour was observed for five of the six individual structures. Only the volumes of the posterior cingulate gyrus did not differ among any of the PCA groups, although there was a trend, mainly driven by the subtle difference between PCA-0 and PCA-2. This limited correspondence between PCA rating scale scores and posterior cingulate gyrus volumes is in line with an earlier report where higher PCA scores only moderately corresponded with smaller volumes of the posterior cingulate gyrus [7]. The authors hypothesised that PCA might reflect more than posterior cingulate atrophy alone, which is confirmed by our current findings as the other five anatomical structures did show the expected relation with PCA scores. Another explanation may be that the anatomical proximity of the posterior cingulate gyrus, especially to the retrosplenial cortex and precuneus, makes it rather difficult to assess visually, although limiting its contribution to the PCA score determined by the rater. Finally, the posterior cingulate gyrus is a very small structure, making it more prone to registration errors than larger regions, possibly increasing variability among subjects.

Third, VBM analyses showed that the visual PCA rating scale discriminates well between atrophy and no atrophy in the parietal brain regions considered by the rating scale. The visual PCA rating scale also discriminates well between minimal atrophy and moderate/severe atrophy, reflecting that higher visual rating scale scores correspond to a specific pattern of atrophy in the posterior cortex. The VBM findings complement the volumetric measurements with more anatomical detail. Nevertheless, the volumetric measurements revealed differences among the minimal, moderate, and severe atrophy groups separately, whereas VBM only detected significant differences in the parietal brain regions when comparing PCA-1 with PCA-2 and PCA-3 together. This may be due to differences among atrophy patterns in individual patients: atrophic regions that do not overlap precisely may go unnoticed by VBM but can be detected when quantifying GM volumes in larger ROIs. Our three-level analysis suggests that higher PCA scores are related to smaller posterior GM volumes, with probably some (limited) variation between patients as regards the exact anatomical distribution of those atrophic changes.

Voxel-based morphometry analyses also showed that in this subject group, increasing PCA scores corresponded to more GM atrophy in other brain regions. This finding is driven by the composition of our study group, which is a representative sample of patients attending a memory clinic, and emphasises that isolated atrophy of the posterior cortex is an exception.

The discrimination between no and mild atrophy (PCA-0 vs. PCA-1), as well as the discrimination between mild and moderate/severe atrophy (PCA-1 vs. PCA-2/3), was driven mainly by the inferior parietal gyrus volume, which thus seems to play a major role in the visual scoring of PCA. Inferior parietal gyrus volume was related to cognitive status and predictive of future AD development in a previous study [5]. This is in line with our findings, as the higher the score, the more AD patients are categorised into the PCA groups, making the inferior parietal gyrus an import subregion of the PCA spectrum. In addition to the inferior parietal gyrus, the precuneus was found to contribute to the discrimination between rating scores 0 and 1, which is not surprising as it is one of the largest structures in the region. Finally, the angular gyrus contributed to the distinction between 0 and 1, and between 1 and 2. It should be noted that in both cases the effect was reversed because of collinearity.

A strength of this study was the comprehensive approach with three levels of anatomical detail, including a carefully applied VBM pipeline with visual checks at each step, allowing clear quantitative and visual validation of the PCA rating scale. A possible limitation of this study is that only one rater rated most of the MRI examinations. To ensure that our results can be generalised, our study protocol included an additional rating by another rater of 10 % of all acquisitions (each tenth consecutive acquisition), as well as of all acquisitions where there was doubt about the scoring. The inter-rater reliability between the two raters was very high with a weighted kappa (quadratic weights) of 0.85 for left and right scores, indicating the generalisability of our results. Another possible limitation is that, strictly speaking, the visual rating scale by definition also assesses the widening of the sulci in the posterior region. However, widening of the sulci is difficult to quantify reliably as the inner boundary of the skull is notoriously difficult to detect on 3D T1 images owing to the limited contrast between bone and CSF. Nevertheless, GM atrophy is supposed to underlie the widening of the sulci, which was reliably measured in this study. In order to limit the number of patient groups in our comparisons, and because most of the patients had equal PCA rating scores for their left and right hemispheres, we only included subjects with symmetric PCA rating scores. Nevertheless, there does not appear to be a plausible biological reason why the current validation of the PCA rating scale would not generalise to asymmetric scores. In spite of the large total number of patients (357), there were only 13 patients in the PCA-3 group, hampering the detection of any putative GM volume differences with the PCA-2 group because of low statistical power.

The findings of the current study have important implications. As PCA has been shown to be an additional marker for AD and helps distinguish AD from FTD, it is important to use the visual rating scale in daily practice. We demonstrated that the visual rating scale for PCA reliably reflects GM atrophy in posterior regions. Because alternative approaches involving quantitative image post-processing techniques are time-consuming, require sophisticated post-imaging analysis, and may be variable across pulse sequences, the simplicity of this

visual rating scale has a great advantage for clinical practice, making it a useful tool in the daily radiological assessment of dementia.

All patients were also included in a recent paper on grey matter differences between early- and late-onset Alzheimer's disease with an unrelated use of the same imaging data (Möller et al. Different patterns of grey matter atrophy in early- and late-onset Alzheimer's disease. Neurobiol Aging 2013; 34:2014-2022 PubMed).

References

1. Scheltens P, Fox N, Barkhof F, DeCarli CD (2002) Structural magnetic resonance imaging in the practical assessment of dementia: beyond exclusion. Lancet Neurol 1:13–21
2. Sluimer JD, Vrenken H, Blankenstein MA et al (2008) Whole-brain atrophy rate in Alzheimer disease: identifying fast progressors. Neurology 70:1836–1841
3. Karas G, Scheltens P, Rombouts S et al (2007) Precuneus atrophy in early-onset Alzheimer's disease: a morphometric structural MRI study. Neuroradiology 49:967–976
4. Benson DF, Davis RJ, Snyder BD (1988) Posterior cortical atrophy. Arch Neurol 45:789–793
5. Jacobs HI, Van Boxtel MP, Uylings HB, Gronenschild EH, Verhey FR, Jolles J (2011) Atrophy of the parietal lobe in preclinical dementia. Brain Cogn 75:154–163
6. Lehmann M, Rohrer JD, Clarkson MJ et al (2010) Reduced cortical thickness in the posterior cingulate gyrus is characteristic of both typical and atypical Alzheimer's disease. J Alzheimers Dis 20:587–598
7. Lehmann M, Koedam EL, Barnes J et al (2012) Posterior cerebral atrophy in the absence of medial temporal lobe atrophy in pathologically-confirmed Alzheimer's disease. Neurobiol Aging 33: 627.e1–627.e12
8. Koedam EL, Lehmann M, van der Flier WM et al (2011) Visual assessment of posterior atrophy development of a MRI rating scale. Eur Radiol 21:2618–2625
9. Scheltens P, Launer LJ, Barkhof F, Weinstein HC, van Gool WA (1995) Visual assessment of medial temporal lobe atrophy on magnetic resonance imaging: interobserver reliability. J Neurol 242:557–560
10. Bresciani L, Rossi R, Testa C et al (2005) Visual assessment of medial temporal atrophy on MR films in Alzheimer's disease: comparison with volumetry. Aging Clin Exp Res 17:8–13
11. Davies RR, Scahill VL, Graham A, Williams GB, Graham KS, Hodges JR (2009) Development of an MRI rating scale for multiple brain regions: comparison with volumetrics and with voxel-based morphometry. Neuroradiology 51:491–503
12. McKhann G, Drachman D, Folstein M, Katzman R, Price D, Stadlan EM (1984) Clinical diagnosis of Alzheimer's disease: report of the NINCDS-ADRDA Work Group under the auspices of Department of Health and Human Services Task Force on Alzheimer's Disease. Neurology 34:939–944
13. Petersen RC, Stevens JC, Ganguli M, Tangalos EG, Cummings JL, DeKosky ST (2001) Practice parameter: early detection of dementia: mild cognitive impairment (an evidence-based review). Report of the Quality Standards Subcommittee of the American Academy of Neurology. Neurology 56:1133–1142
14. Fazekas F, Chawluk JB, Alavi A, Hurtig HI, Zimmerman RA (1987) MR signal abnormalities at 1.5 T in Alzheimer's dementia and normal aging. AJR Am J Roentgenol 149:351–356
15. Pasquier F, Leys D, Weerts JG, Mounier-Vehier F, Barkhof F, Scheltens P (1996) Inter- and intraobserver reproducibility of cerebral atrophy assessment on MRI scans with hemispheric infarcts. Eur Neurol 36:268–272
16. Jenkinson M, Smith S (2001) A global optimisation method for robust affine registration of brain images. Med Image Anal 5:143–156
17. Alemán-Gómez Y, Melie-García L, Valdés-Hernandez P (2006) IBASPM: toolbox for automatic parcellation of brain structures. Presented at the 12th Annual Meeting of the Organization for Human Brain Mapping, Florence, Italy. Available on CD-Rom in. 27 ed, 2006. 11-15 June
18. Tzourio-Mazoyer N, Landeau B, Papathanassiou D et al (2002) Automated anatomical labeling of activations in SPM using a macroscopic anatomical parcellation of the MNI MRI single-subject brain. Neuroimage 15:273–289
19. Ashburner J (2007) A fast diffeomorphic image registration algorithm. Neuroimage 38:95–113
20. Frisoni GB, Pievani M, Testa C et al (2007) The topography of grey matter involvement in early and late onset Alzheimer's disease. Brain 130:720–730
21. Barnes J, Godbolt AK, Frost C et al (2007) Atrophy rates of the cingulate gyrus and hippocampus in AD and FTLD. Neurobiol Aging 28:20–28